Multiple preequilibrium emission in Feshbach-Kerman-Koonin analyses

M. B. Chadwick
University of California, Nuclear Data Group, Lawrence Livermore National Laboratory, Livermore, California 94551

P. G. Young and D. C. George
University of California, Theoretical Division, Los Alamos National Laboratory, Los Alamos, New Mexico 87545

Y. Watanabe
Department of Energy Conversion Engineering, Kyushu University, Kasuga, Fukuoka 816, Japan
(Received 21 March 1994)

We describe how multiple preequilibrium emission can be included in the Feshbach-Kerman-Koonin (FKK) theory. By analyzing (p, xn) and (p, xp) reactions on zirconium, at incident energies of 80 and 160 MeV, the importance of multiple preequilibrium emission can be clearly seen. This mechanism accounts for much of the emission spectra and its importance extends to relatively high emission energies. We show that multiple preequilibrium must be included in FKK analyses at these incident energies in order to simultaneously satisfy unitarity and account for inclusive nucleon emission spectra. The importance of multistep processes is reduced in comparison to analyses which omit multiple preequilibrium. Our calculated angular distributions account for measurements except at the highest backward angles, where we underpredict the data. We compare our results with other analyses at these energies.

PACS number(s): 24.60.Gv, 24.60.Dr, 25.40.Ep, 24.50.+g

I. INTRODUCTION

The multistep scattering theory of Feshbach, Kerman, and Koonin [1] can be used to calculate preequilibrium cross sections for nucleons incident on a nucleus with energies up to the pion threshold. The theory is particularly attractive since it combines a quantum mechanical approach to multistep scattering with statistical assumptions that readily allow numerical cross section calculations, and this has resulted in much recent work on its application to the analysis of experimental measurements [2–5] and to nuclear data evaluation [6–11]. However, the theory as it was originally formulated only takes into account the preequilibrium emission of one particle (primary preequilibrium emission), with the assumption that this particle carries away so much energy that the remaining excited residual nucleus cannot emit another preequilibrium particle, and instead becomes equilibrated before undergoing compound nucleus decay. For nucleon-induced reactions with incident energies above a few tens of MeV this assumption begins to fail, and it is possible to emit more than one particle through a preequilibrium mechanism (multiple preequilibrium emission). It is the purpose of this paper to describe how multiple preequilibrium emission can be included in FKK analyses.

It has long been recognized that multiple preequilibrium processes are important in inelastic reactions above a few tens of MeV incident energy. Akkermans and Gruppelaar [12] incorporated them in the semiclassical exciton model, and Blann [13] included them in his semiclassical hybrid model. These models picture the nuclear reaction as passing through a series of particle-hole states toward equilibrium, particle decay from these states giving the high energy emission. After the first preequilibrium particle is emitted, the residual nucleus is left with particle-hole excitations which may subsequently particle decay to give multiple preequilibrium emission. In addition to these two semiclassical models, the intranuclear cascade model includes processes in which a number of high-energy particles can be emitted during the early stages of the reaction. Also, Fortsch *et al.* [14] recently considered the quasifree knockout of two protons in proton-induced reactions and stressed the need to extend multistep-direct theories to include two-particle emission. It is therefore a natural development to include multiple preequilibrium processes in the FKK theory. A formalism for multiparticle emission processes which makes physical assumptions similar to those of FKK has been developed by Ciangaru [15]. However, this formalism does not readily lend itself to numerical computations [16]. Our approach, on the other hand, is straightforward to implement, does not introduce any free parameters, and makes use of DWBA matrix elements already determined for primary preequilibrium emission. According to the FKK theory two types of preequilibrium emission can occur: multistep direct (MSD) and multistep compound (MSC), depending on whether the preequilibrium stages contain unbound or bound particle excitations. Since MSC processes are only important for incident energies below about 30 MeV [17] we concentrate here on the MSD mechanism. A formalism for multiple MSC emission has been developed [18] though it is of limited practical importance.

In this paper we investigate the importance of primary and multiple MSD by analyzing emission spectra from $^{90}\mathrm{Zr}(p, n)$ and $^{90}\mathrm{Zr}(p, p')$ reactions at incident proton energies of 80 and 160 MeV. At these energies both

neutron and proton emission differential cross section measurements are available, from the Indiana University Cyclotron Facility and the National Accelerator Laboratory at Faure, respectively, allowing an extensive test of our model. The recent papers by Koning and Akkermans [6] and by Richter *et al.* [4] on MSD reactions highlighted the possible importance of multiple particle emission at the lowest emission energies. We shall show that by satisfying unitarity (and thus forbidding the total summed primary preequilibrium cross sections from exceeding the optical model reaction cross section) the importance of multiple preequilibrium emission can be clearly seen, even for relatively high emission energies.

For this analysis we use the FKK-GNASH code system [7–10], which applies the FKK theory for preequilibrium emission and Hauser-Feshbach theory for equilibrium decay. We account for all reaction decay sequences that contribute to the inclusive nucleon emission spectra, over the whole emission energy range. This is important since the conclusions we draw from comparisons between theory and experiment are dependent on a complete description of all contributing processes, and at low emission energies both multiple preequilibrium and equilibrium contributions can be large.

Accurate modeling of proton reactions at intermediate energies is of practical importance in applications ranging from accelerator shielding design to the accelerator-based transmutation of nuclear waste [19, 20]. To assess the accuracy of nuclear model codes at these energies, these same reactions on zirconium were the subject of a recent code intercomparison, organized by the Nuclear Energy Agency of the OECD [21]. Using the FKK-GNASH code system we participated in this intercomparison, and pointed to the importance of multiple preequilibrium emission [8, 10]. However, although our calculations for primary MSD used the FKK theory, the multiple emission cross sections in this earlier work were obtained semiclassically with the exciton model.

In Sec. II A we describe our implementation of FKK primary MSD emission, emphasizing aspects which differ from other works, and in Sec. II B we describe our FKK multiple MSD emission model. Details of our Hauser-Feshbach compound nucleus calculations for equilibrium decay are given in Sec. II C. We apply our model to describe proton reactions on zirconium in Sec. III, comparing our calculations with measurements, and give our conclusions and suggestions for future work in Sec. IV.

II. THEORY

A. Primary MSD preequilibrium emission

The full primary MSD emission cross section is an incoherent sum of contributions from the various preequilibrium stages (labeled by N). The one-step cross section plays a crucial role in the theory since cross sections from the Nth preequilibrium stage are expressed as a series of one-step scatterings. It is obtained by extending DWBA theory into the continuum, and for a projectile of incident energy E_0 and angle Ω_0 and ejectile of energy E and angle Ω, is given by [9]

$$\frac{d^2\sigma^{(1)}(E,\Omega \leftarrow E_0,\Omega_0)}{d\Omega dE} = \sum_J \frac{(2J+1)}{(2I+1)(2i+1)} \sum_{S_f=0}^{1} \frac{1}{(2S_f+1)} \times \sum_{S=|I-S_f|}^{I+S_f} \sum_{l=|J-S|}^{J+S} \rho(1p,1h,U,l) \left\langle \left[\frac{d\sigma(E,\Omega \leftarrow E_0,\Omega_0)}{d\Omega} \right]_l^{\mathrm{DWBA}} \right\rangle , \quad (1)$$

where p and h are the number of particles and holes excited, and l is the orbital angular momentum transfer. J, I, and i are the residual nucleus, target, and nucleon intrinsic spins, respectively, and S_f=0 or 1 is the spin-flip. $\left\langle \left[d\sigma(E,\Omega \leftarrow E_0,\Omega_0)/d\Omega \right]_l^{\mathrm{DWBA}} \right\rangle$ is the average of DWBA cross sections exciting $1p1h$ states consistent with energy, angular momentum, and parity conservation. The density of such states with residual nucleus energy U ($=E_0-E+Q$, where Q is the reaction Q value) can be partitioned into the energy-dependent density multiplied by a spin distribution, $\rho(p,h,U,l) = \omega(p,h,U)\ R_n(l)$. We use the Williams [22] equidistant expression with finite hole-depth restrictions for the energy dependent density,

$$\omega(p,h,U) = \frac{g^n}{p!h!(n-1)!} \sum_{j=0}^{h} (-1)^j \binom{h}{j} (U - \Delta - A_{ph} - j\epsilon_F)^{n-1} \Theta(U - \Delta - A_{ph} - j\epsilon_F), \quad (2)$$

where $n = p + h$, g is the single particle density, ϵ_F is the Fermi energy, Δ is the pairing energy, and $A_{ph} = p^2 + h^2 + p - 3h/4g$ accounts for Pauli blocking. The Θ function is unity if its argument is positive, and zero otherwise. With the finite well-depth restriction the $1p1h$ phase space ceases to rise linearly with U for excitation energies above the Fermi energy, and instead remains constant. Previous MSD calculations ignore finite hole-depth restrictions and significantly overestimate this phase space for residual nucleus energies above about 40 MeV. A Gaussian spin distribution is adopted,

$$R_n(l) = \frac{2l+1}{2\sqrt{2\pi}\sigma_n^3} \exp\left[-\frac{(l+1/2)^2}{2\sigma_n^2} \right], \quad (3)$$

where σ_n is the spin cut-off parameter.

At present there is no consensus among practitioners of the FKK theory as to whether normal or both normal and non-normal DWBA matrix elements should be used for the multistep transitions [23, 24, 9]. In this paper we follow Feshbach [23] in using normal DWBA matrix elements, though we are currently investigating the alternative approach. Multistep cross sections are then given by a convolution of one-step cross sections, the contribution from the Nth stage being

$$\frac{d^2\sigma^{(N)}(E,\Omega \leftarrow E_0,\Omega_0)}{d\Omega dE} = \frac{m}{4\pi^2\hbar^2}\int d\Omega_{N-1}\int dE_{N-1}E_{N-1} \times \frac{d^2\sigma^{(1)}(E,\Omega \leftarrow E_{N-1},\Omega_{N-1})}{d\Omega dE}\ \frac{d^2\sigma^{(N-1)}(E_{N-1},\Omega_{N-1} \leftarrow E_0,\Omega_0)}{d\Omega_{N-1}dE_{N-1}}. \quad (4)$$

V_0 is the only free parameter entering the MSD calculations, and is extracted by varying it until the highest-energy emission spectrum data (where the multiple preequilibrium contribution is negligible) is described. It is not simply a normalization parameter, however, since different steps depend on different powers of V_0, and thus its value determines the overall shape, as well as the magnitude [25]. In our calculations we account for MSD emission at all emission energies, and in our determination of V_0 we always ensure that the integrated primary preequilibrium spectra, summed over all decay channels, does not exceed the reaction cross section obtained from the optical model.

For the incident energies considered here, our approach for determining V_0 leads to a primary MSD spectrum that lies below experimental data at all but the highest emission energies, and we find that multiple preequilibrium emission, and equilibrium emission, accounts for the difference.

B. Multiple preequilibrium emission

Various aspects of multiple preequilibrium decay have been reviewed by Blann [26], who paid particular attention to its dramatic influence on $(p,2p)$ excitation functions for incident energies to 90 MeV. Recently, similar effects have been established for the ^{208}Pb$(n,2n\gamma)$ excitation function [27], obtained from the LAMPF/WNR white neutron source for neutron energies to 200 MeV. In both these cases the inclusion of multiple preequilibrium increases the calculated excitation functions by orders of magnitude, and this is easy to understand: Multiple preequilibrium provides a mechanism by which two high-energy particles can be emitted, leaving a residual nucleus with a sufficiently low excitation energy for further particle decay to be prohibited. The increase in the nucleon emission spectra due to multiple preequilibrium emission is less dramatic, though still large. For instance, the semiclassical analyses of proton reactions on zirconium and lead in the recent NEA code intercomparison, using the GNASH and ALICE codes, both needed multiple preequilibrium to adequately account for measurements [21]. We shall address the issue of multiple preequilibrium FKK analyses of excitation functions in a future paper, but here we concentrate on its influence on inclusive emission spectra.

When describing multiple preequilibrium emission, we use the notation that "stage" refers to the exciton class from which the emission occurs, see Fig. 1. Thus, if primary MSD emission occurs from the first stage, leaving a $1p1h$ excitation, subsequent immediate particle emission from this configuration is referred to as first stage multiple preequilibrium emission. Blann [13] identified two types of multiple preequilibrium decay: "type I," in which more than one excited particle is emitted from a single exciton class; and "type II," in which a particle is emitted, after which a number of intranuclear (damping) transitions occur, and then a second preequilibrium particle is emitted. He showed that type II processes are relatively unimportant compared to type I. Our calculation of type II processes in the FKK theory confirm this. We treated [18] such processes in which an emission occurs, followed by a scattering and another emission, in the spirit of FKK by convoluting two scatterings, though we obtained small cross sections. Thus it is the type I multiple emissions that we consider here.

The original FKK restriction to only one preequilibrium particle limits the theories applicability to incident energies below about 50 MeV, unless one concentrates solely on small energy-transfer inelastic scattering. In previous FKK calculations the question of how to treat multistep reactions leaving residual nuclei in highly excited states, where particle excitations may be in the continuum, has been solved by (somewhat artificially) making such particles quasibound [28]. This then facilitates the use of a DWBA code such as DWUCK4 [29] to determine matrix elements for particle-hole creation, without the need to use a code which can treat more than one continuum particle exactly.

Our approach uses this same method to determine the

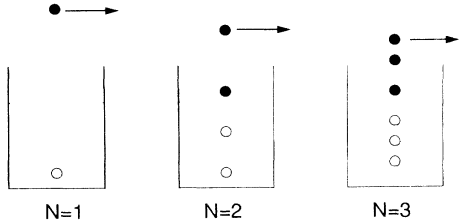

FIG. 1. Multiple preequilibrium emission from various particle-hole preequilibrium stages.

primary preequilibrium emission cross sections. But in addition, we consider type I processes in which a second particle is emitted from a preequilibrium stage. An important element of our approach is the realization that the MSD calculational procedure as described in Sec. II A (originally intended solely for primary MSD calculations) contains a large part of the effort needed to calculate the subsequent type I multiple emission. This is because processes in which a continuum particle is left after primary preequilibrium emission are already included in Eq. (1) (the phase space includes these configurations), and the probability of subsequent emission of such particles would be expected to be high, unless they are of low energy. To calculate cross sections for these processes we follow Weidenmuller's suggestion [30] that the probability for two continuum particles being emitted can be approximated by multiplying the results obtained using the above procedure with a transmission coefficient, which describes the probability that the second particle escapes from the nucleus rather than undergoes damping interactions. All the particles in the continuum are treated on an equal footing, without distinguishing a leading particle, which is necessary for cases in which the energy loss in scattering is substantial. Our approach allows multiple emission to be determined within the existing FKK formalism and does not require the determination of any additional DWBA matrix elements. For clarity we only consider processes in which up to two preequilibrium particles are emitted, which should be sufficient for reactions induced by nucleons with energies up to 160 MeV [26], though our formalism can be easily generalized to include more emissions.

To determine the cross section for emission of a second preequilibrium particle at an energy E, we start with the cross section for producing particle-hole states of a certain energy U after primary preequilibrium emission, and determine the probability that among such states there exists a nucleon at the energy of interest ($E+B$ relative to the Fermi level, where B is the separation energy) which can escape with transmission-coefficient probability. To do this we make the simplifying assumption (also made in semiclassical preequilibrium models) that all possible exciton configurations in a given p-h class are equiprobable. In Fig. 2 we give an example of multiple preequilibrium emission from the $1p1h$ stage. The angle-integrated spectrum of multiple preequilibrium emission is then given as a sum of contributions from each preequilibrium stage N (where $p{=}h{=}N$ before emission),

$$\frac{d\sigma_{\rm mul}^{(j)}}{dE} = \sum_N \frac{d\sigma_{\rm mul}^{(N,j)}}{dE}$$

where

$$\frac{d\sigma_{\rm mul}^{(N,j)}}{dE} = \sum_{i=\pi,\nu} \int_{U=E+B}^{U_{\rm max}} \frac{d\sigma^{(N,i)}}{dU} \left[\frac{1}{p} \frac{\omega(1p,0,E+B)\omega(p-1,h,U-E-B)}{\omega(p,h,U)} R_N^{i,j} \right] T_j(E)\, dU \ , \tag{5}$$

where E is the emission energy, i labels the type of primary-emitted particle [π = proton, ν = neutron], and j labels the multiple preequilibrium particle type. $d\sigma^{(N,i)}/dU$ is the differential cross section of p-h states after primary preequilibrium emission of a nucleon of type i from stage N as a function of residual nucleus energy, obtained from the angle integration of Eq. (4). Thus, in order to calculate the inclusive proton emission spectrum, for example, both proton and neutron primary preequilibrium spectra must be calculated. The transmission coefficient $T_j(E)$ is the probability that the continuum particle j escapes with an energy E, and for simplicity we take this from the s-wave transmission coefficient from an optical potential. Taking just the s-wave coefficient is certainly an approximation, though it does account for the physically expected behavior of being close to unity for most emission energies, but decreasing for low energies. The inclusion of this term is particularly important for protons, where low energy emission is strongly suppressed by the Coulomb barrier. The quantity in the square brackets represents the probability of finding a particle j at an energy $(E+B)$ inside a p-h exciton configuration of energy U, based on the equiprobability assumption. $R_N^{i,j}$ accounts for neutron-proton distinguishability and is the probability of finding a nucleon of type j in the exciton class N after primary emission of type i. Since we consider only one emission in the multiple preequilibrium process, these numbers yield unity when summed over j for a given i, N. Blann's method (Eqs. (9) and (10) of Ref. [13]) is used to determine these values, using a ratio of the n-p to n-n or p-p cross sections of 3:1.

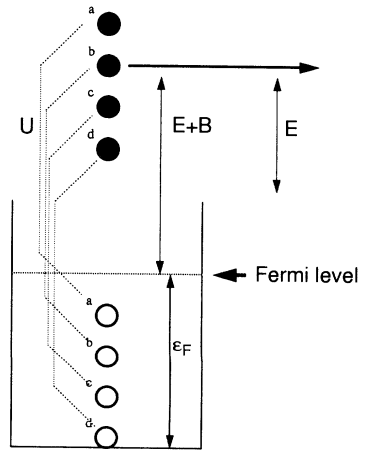

FIG. 2. First stage multiple preequilibrium emission. Various $1p1h$ states, labeled "a" though "d," are shown for a residual nucleus energy U. The excited particle from the p-h pair "b" can be emitted with energy E.

As we treat the excited particles in the preequilibrium cascade on an equal footing, we use the same angular distribution for particles emitted through multiple and primary emission (for the same emission energy), so

$$\frac{d^2\sigma_{\rm mul}^{(N,j)}}{dEd\Omega} = \frac{d\sigma_{\rm mul}^{(N,j)}}{dE}\, G(\Omega \leftarrow \Omega_0)\ , \qquad (6)$$

where the angular kernel is obtained from Eq. (4), $G(\Omega \leftarrow \Omega_0) = \left[d^2\sigma^{(N,j)}/dEd\Omega/d\sigma^{(N,j)}/dE\right]$. If a primary particle is emitted with a high energy, it will tend to be emitted in the forward direction; if a second particle is then emitted it will be of lower energy and less likely to be emitted forward. Thus, the correlated angular effects expected for two particle scattering into the continuum are as would be expected from kinematic considerations.

C. Hauser-Feshbach equilibrium decay

We use Hauser-Feshbach theory to describe compound nucleus decay of equilibrated nuclei, allowing us to describe the emission spectrum down to the lowest energies. These nuclei are formed in one of two ways: either they are produced in the initial interaction when no preequilibrium particles were emitted; or they are residuals after previous preequilibrium or equilibrium emission with sufficient excitation energy to undergo further particle decay. The FKK-GNASH code includes both these types of decay, though at the incident energies considered in this work the second type is most important, since there is sufficient energy for many sequential decays to occur.

The full angular-momentum dependent version of the Hauser-Feshbach model in the GNASH code [31] is incorporated into FKK-GNASH. Any number of reaction decay chains can be included, with limitations arising only from computer time. In the present calculations we included the decays of a total of 33 residual nuclei. Details of our selection of decay sequences are given in the next section. Transmission coefficients needed for particle decay calculations are obtained with the SCAT2 code [32], and for all decaying nuclei considered a continuum level density description is matched on to the known low-lying nuclear structure.

Unitarity, or reaction flux conservation, is automatically satisfied in our calculations, and in the next section we stress the importance of this for the primary emitted particles. But in Ref. [7] we also showed how such considerations point to the existence of crossover transitions from the MSD to MSC chains ("$P \rightarrow Q$ transitions"). At the high energies considered here, only a relatively small amount of the reaction flux survives to equilibrium without suffering preequilibrium decay. But since it is energetically impossible to form a bound MSC $2p1h$ doorway state for incident energies of 80 and 160 MeV, this flux must have come from $P \rightarrow Q$ transitions, and such transitions are implicitly included in our paper.

III. RESULTS

A. Calculational details and input parameters

When calculating MSD cross sections with Eqs. (1) and (4), we used the following default input parameters: the single-particle level density was taken as $g = A/13$ MeV^{-1}; the pairing energy as zero; the Fermi energy as ϵ_F=40 MeV; and the spin cut-off as $\sigma_n^2 = 0.24nA^{2/3}$ [33]. To calculate the DWBA matrix elements, we used a Yukawa potential of range 1 fm, with bound wave functions from a Wood-Saxon potential and unbound wave functions from optical scattering states. These were obtained from the Walter-Guss [34] optical potential for energies below 50 MeV. Above 50 MeV we used the global Madland-Schwandt medium energy potential. This potential was based on proton scattering work of Schwandt [35] and was extended by Madland [36] to higher energies and to include neutrons, with a primary emphasis on reproducing integrated scattering observables (neutron total cross sections and proton reaction cross sections), and secondarily on reproducing the angular-dependent scattering observables.

The code DWUCK4 [29] is a subroutine in FKK-GNASH, and with it many microscopic DWBA cross sections are calculated and averaged, in accordance with Eq. (1). Typically we average about 30 different microscopic transitions for each residual nucleus energy. Particle-hole quantum numbers for each state that can be excited were obtained from a spherical Nilsson shell model scheme [37], allowing an energy spread of $\pm$ 3 MeV away from the exact energy obtained from energy conservation. Physically this accounts for the fact that the true eigenvalues can deviate considerably from those given by the spherical Nilsson model due to shape deformation, as well as having a finite width, and computationally has the result that our calculated emission spectrum varies smoothly with emission energy, in agreement with experimental measurements. The energy eigenvalues of the particle and hole are input, and DWUCK4 searches on the potential well depth to obtain the eigenfunctions.

When calculating multistep MSD cross sections with Eq. (4), it is clear that we need one-step cross sections at the incident energy as well as at all lower energies. In practice this is done by determining one-step cross sections at five lower energies in addition to the true incident energy, and interpolating for other values. We have found that the square of the residual interaction strength varies approximately inversely with incident energy [7, 10], and therefore incorporate this energy dependence into our multistep calculations in Eq. (4). We solve this three-dimensional equation using Monte Carlo numerical integration.

The preequilibrium emission of deuteron and alpha clusters can be significant, as was found in the proton-induced measurements of Bertrand and Peelle [38]. We therefore include these decay channels, and use Kalbach's [31, 39] reaction model for direct cluster emission to the continuum.

Before performing the Hauser-Feshbach analysis, trial calculations were performed with 160 MeV protons incident on ^{90}Zr to determine the reaction sequences that make significant (σ greater than $\sim$ 1 mb) contributions to the proton and neutron emission spectra. The decay sequence used in the calculation includes neutron, proton, and γ-ray decay for Nb isotopes from ^{91}Nb through ^{85}Nb, for Zr isotopes from ^{90}Zr through ^{85}Zr, for Y iso-

topes from ^{89}Y through ^{83}Y, for Sr isotopes from ^{88}Sr through ^{82}Sr, and for Rb isotopes from ^{87}Rb through ^{82}Rb. Additionally, alpha particle and deuteron emission was included for the primary channel. No other reactions produce significant contributions to the neutron or proton emission spectra.

Level densities were obtained from the Ignatyuk [40] phenomenological model, which includes energy-dependent shell effects, utilizing the parametrization of Arthur (see Ref. [31]) for the level density parameters. The spherical optical model potentials of Arthur [41] based on an analysis of neutron and proton reactions on ^{89}Y and ^{90}Zr, was matched above 20 MeV with the global parametrization of Madland [36] and was used to calculate proton and neutron transmission coefficients. A medium energy complex particle potential [36], based on the approach of Watanabe [42], was used for the deuteron and alpha particle transmission coefficients. Estimates of gamma-ray competition were made using gamma-ray strength functions from the generalized Lorentzian model of Kopecky and Uhl [43].

B. Comparison with inclusive emission spectra

In Fig. 3 we show the theoretical primary and multiple MSD contributions to the inclusive angle-integrated neutron spectrum in the reaction ^{90}Zr(p,n) for an incident energy of 160 MeV. At the highest emission energies, one- and two-step primary MSD dominate, though the multiple MSD from the first stage is also important. Multiple emission processes are seen to be important over almost the whole energy range. As would be expected, the major contribution from multiple MSD at high emission energies comes from the first stage, where a $1p1h$ state decays by particle emission. This process is equivalent to a knockout mechanism in which the incident proton strikes a bound neutron, and both particles are emitted leaving a neutron hole. Note that the hard spectral shape of first stage (N=1) multiple MSD seen in Fig. 3 results from the finite hole-depth restrictions in Eq. (2) when applied in Eq. (5) [44]. For more complex particle-hole excitations the probability of there being an excited particle at a high energy is reduced, and hence the cross sections for multiple MSD emission from later stages are correspondingly smaller.

In Figs. 4–7 we show comparisons between theoretical predictions and experimental measurements of angle-integrated neutron and proton emission spectra for proton reactions on zirconium at 80 and 160 MeV. The solid curves represent our calculations including all reaction mechanisms contributing to the inclusive spectra. The contribution from primary MSD is shown by the dashed line, multiple MSD by the dashed-dot line, and Hauser-Feshbach equilibrium decay by the dotted line. The primary and multiple MSD spectra shown are summed over the various preequilibrium stages. It is evident that the calculations account for the measurements well, for both neutron and proton emission. The importance of multiple preequilibrium emission can be clearly seen for all emission energies except the very highest, and at the lower emission energies this mechanism accounts for much of the data. The multiple preequilibrium contribution does not extend as high in emission energy as the primary contribution, because of the separation energy expended in emitting a second nucleon. Nucleons emitted at the highest energies through the multiple preequilibrium mechanism follow the primary preequilibrium emission of a low energy nucleon. Without multiple preequilibrium the FKK theory would underestimate the data at all but the highest emission energies. The measurements do not extend low enough in emission energy to test the Hauser-Feshbach contribution, which is already negligible where data exist. The experimental measurements approximately follow the systematics of Kalend *et al.* [45], who noted that in proton-induced reactions at 90 MeV the proton yields are about twice the neutron yields above the evaporation region, and our calculations match these systematics.

In Fig. 8 we show theoretical angular distributions compared with data for the 80 MeV ^{90}Zr(p,xp) reac-

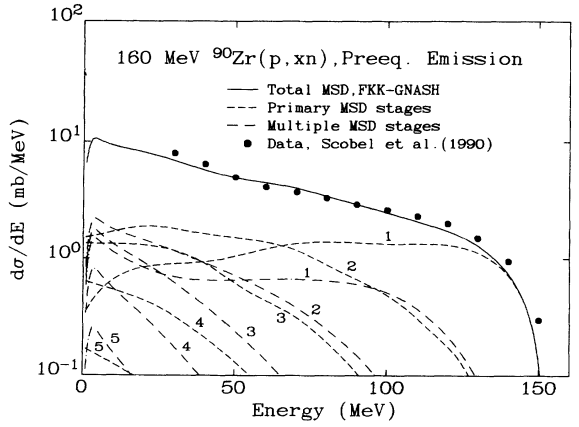

FIG. 3. Angle-integrated contributions, calculated with FKK-GNASH, from various preequilibrium stages in primary and multiple MSD in the 160 MeV ^{90}Zr(p,xn) reaction. Experimental measurements by Scobel *et al.* [48] are also shown for comparison.

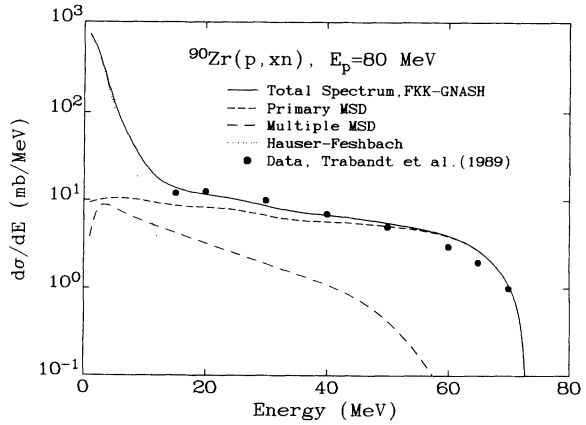

FIG. 4. FKK-GNASH calculation of the 80 MeV inclusive ^{90}Zr(p,xn) angle-integrated spectrum, compared with experimental measurements of Trabandt *et al.* [46].

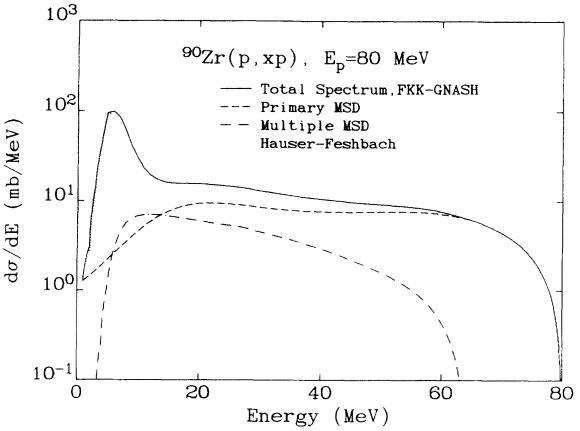

FIG. 5. FKK-GNASH calculation of the 80 MeV inclusive ^{90}Zr(p, xp) angle-integrated spectrum. Experimental angle-integrated measurements have not been published for this reaction. See Fig. 8 for a comparison with double-differential measurements.

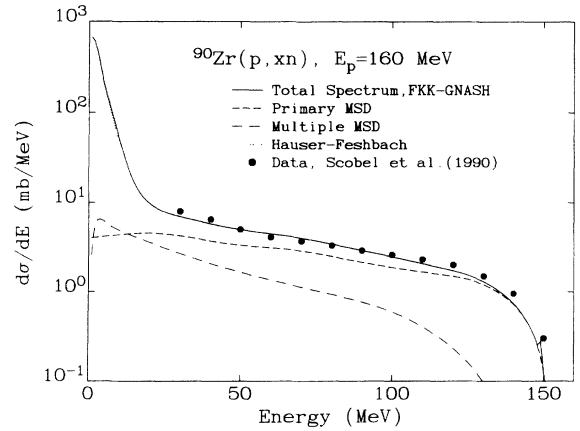

FIG. 6. FKK-GNASH calculation of the 160 MeV inclusive ^{90}Zr(p, xn) angle-integrated spectrum, compared with experimental measurements of Scobel *et al.* [48].

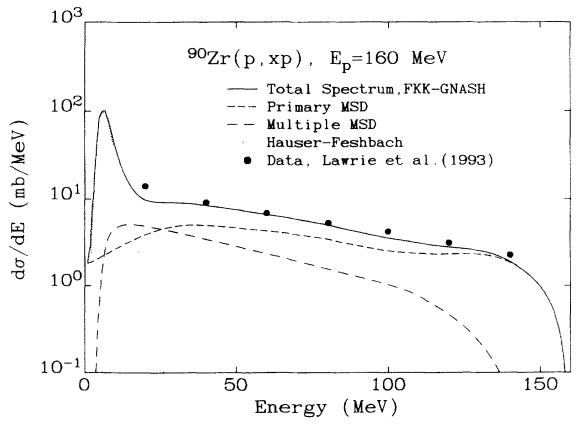

FIG. 7. FKK-GNASH calculation of the 160 MeV inclusive ^{90}Zr(p, xp) angle-integrated spectrum, compared with experimental measurements of Lawrie *et al.* [4].

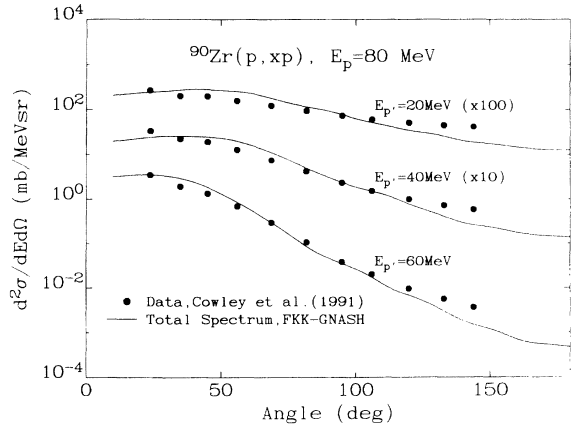

FIG. 8. FKK-GNASH calculation of the 80 MeV ^{90}Zr(p, xp) angular distributions, at proton emission energies of 20, 40 and 60 MeV, compared with experimental measurements of Cowley *et al.* [49]

tion (experimental angle-integrated results have not been published). While the calculations account for the strong forward peaking, and the increasing forward-peaking with emission energy, they underestimate the data at large backward angles. This underestimation has been seen in some other FKK analyses [4, 10] and we address this limitation in more detail in the next subsection. However, the ability of the FKK theory to account for measurements over much of the angular range, and over many orders of magnitude, is impressive.

Values that we obtained for the effective residual interaction strength for the various reactions are shown in Table I, along with the calculated primary preequilibrium integrated cross sections for neutron and proton MSD emission, and deuteron and alpha emission from Kalbach's model. We also show how the primary preequilibrium cross section compares with the reaction cross section from the optical model. In all cases the integrated primary preequilibrium cross section is smaller than the reaction cross section, as it must be if unitarity is satisfied. As would be expected, the probability for preequilibrium decay increases with increasing emission energy, and at the incident energies considered here preequilibrium emission almost exhausts the entire reaction cross section (and hence the ratios of total primary MSD to the reaction cross section in Table I are close to unity). The V_0 values that we obtain in Table I are seen to decrease with increasing incident energy, as first noted by Trabandt *et al.* [46]. The values for (p, p') reactions are about 1.3 times larger than for (p, n) reactions. In our application of the FKK theory we use one-component state densities which do not differentiate neutron and proton excitations. This simplification leads to separate systematics for (p, p') and (p, n) reactions. This is partly due to the fact that in a two-component theory the number of $1p1h$ states that can be excited in a (p, p') scattering is twice that in a (p, n) scattering – and thus if a one-component theory is used, the V_0 value extracted absorbs this difference by becoming $\sqrt{2}$ times larger for (p, p') compared to (p, n) reactions. We stress that this

TABLE I. Values of residual interaction strength and integrated primary MSD cross sections for p+^{90}Zr in this work. In the last column we show the ratio of total primary MSD to the reaction cross section (σ_R=1100 mb at 80 MeV and 942 mb at 160 MeV).

Inc. energy (MeV)	V_0 (MeV) (p,n)	(p,p')	Primary preq. x/s (mb) n	p	d	α	$\sum$ primary preq. $x/s/\sigma_R$
80	11.30	15.00	451	503	70	13	0.943
160	6.52	8.69	396	485	51	9	0.999

strength is "effective" and very much dependent on other parameters used in the theory [47].

C. Comparison with other FKK analyses

A number of other groups have applied the FKK theory to analyze inelastic nucleon scattering at the energies considered in this work, and it is useful to highlight differences between the various approaches. Broadly speaking, the calculational approaches fall into three categories: Those which use the Bonetti and Chiesa code (e.g., Trabandt *et al.* [46], Scobel *et al.* [48], Cowley *et al.* [49], Richter *et al.* [4]) , who were the first to apply the MSD theory at these energies; the work of Koning and Akkermans [6], which uses the KAPSIES code; and our work, which uses the FKK-GNASH code system [7–10, 18]. Below we discuss differences due to multiple preequilibrium processes and their impact on emission spectra, unitarity, angular distributions, and extracted V_0 values.

Calculations using the Bonetti-Chiesa code, and the Koning-Akkermans code have not included multiple preequilibrium emission, and as a consequence have underestimated data at low emission energies [4, 6]. However, our work shows that the importance of multiple preequilibrium extends even to relatively high emission energies, especially for reactions at incident energies as high as 160 MeV. Previous analyses were able to account for much of the observed emission spectra by using an artificially large primary preequilibrium contribution. To see this, we have repeated our analyses using the approach described by Richter [4], who used primary MSD to account for the whole emission spectrum, and chose a V_0 value to fit the experimental data at an emission energy equal to half the incident energy. By doing this, and ignoring multiple preequilibrium emission, we obtain emission spectra which fit the measurements fairly well, but whose integrated value for neutrons and protons exceeds the reaction cross section. We show the V_0 values found in Table II, along with the integrated primary preequilibrium cross sections. In the last column it is seen that such an analysis results in a violation of unitarity by 16% at 80 MeV and 47% at 160 MeV. In contrast, our approach of including multiple preequilibrium does not lead to a breakdown of unitarity, as can be seen from Table I. By comparing the V_0 values in Tables I and II we also see that the previous MSD calculational procedure leads to higher residual interaction strengths. But since multistep processes depend on V_0 to a high power, the extracted values in Tables I and II are only slightly different.

Our work describes the angular distributions fairly well, though we underpredict the data at the largest backward angles. This underprediction is worse in our calculations compared to previous works. The reason for this follows (in part at least) from the above paragraph, since by using a smaller V_0 the relative importance of higher stages decreases (the magnitude of the Nth stage is approximately proportional to V_0^{2N}). Since the angular distribution becomes less forward-peaked as N increases, our approach leads to fewer MSD stages being important, and a more forward-peaked angular distribution results. We are currently investigating whether any modifications to our application of the FKK theory can improve the backward-angle predictions.

The energy dependence of the V_0s we obtain, between 80 and 160 MeV, is in agreement with the results of Scobel *et al.* [48] and Cowley *et al.* [49] though the magnitudes are different. This is due to different input parameters in the various calculations, which ultimately affect the value of V_0 that is extracted. For instance, as mentioned above we use a one-component state density [Eq. (2)], whereas the Bonetti-Chiesa code makes some two-component approximations and treats neutrons and protons separately [47]. We prefer to use the one-component approach until a full two-component formalism has been developed, which uses two-component state

TABLE II. Results obtained if no multiple preequilibrium is included (as in previous MSD analyses). The values in the last column exceed unity and are therefore unphysical. See Table I caption.

Inc. energy (MeV)	V_0 (MeV) (p,n)	(p,p')	Primary preq. x/s (mb) n	p	d	α	$\sum$ primary preq. $x/s/\sigma_R$
80	12.15	16.00	565	624	70	13	1.156
160	7.10	9.60	558	770	51	9	1.473

densities and includes different p-p and p-n interactions. Also, we use a default set of parameters in all calculations and do not treat quantities such as the spin cut-off as adjustable parameters. The energy dependence that we find for V_0 varies approximately as $V_0^2 \propto 1/E_{\rm inc}$, as was found in our earlier work at lower energies [7]. While this variation is similar in shape to that in Refs. [4, 5, 48, 49] between 80 and 160 MeV, it differs considerably at lower energies. Part of this difference may arise because we fold in an energy-dependent V_0 into our multistep calculations, but it could also be because the analyses in Refs. [4, 5, 48, 49] for incident energies above 80 MeV used different input parameters to the earlier MSD analyses below 50 MeV.

IV. CONCLUSIONS AND FUTURE WORK

We have presented a formalism for determining multiple preequilibrium emission which is parameter-free, straightforward to implement, and which makes use of quantities already calculated for primary MSD. Our calculations describe neutron and proton emission spectra well and showed the importance of multiple preequilibrium not only at low emission energies, but also at fairly high emission energies. Without this mechanism it is not possible to simultaneously satisfy unitarity and account for emission spectra. We conclude that it is essential to incorporate multiple preequilibrium into FKK analyses of nucleon-induced reactions when the incident energy exceeds about 50 MeV. We have tested our theory against inclusive nucleon emission spectra measurements. In the future it would be useful to test it against excitation functions such as the $(n, 2n)$ reaction to a specific residual nucleus, which is also very sensitive to multiple preequilibrium emission.

The theory we have presented for multiple preequilibrium emission emphasized computational simplicity and was derived to allow straightforward estimates of these cross sections. There is still a need for a theory based on a rigorous derivation and which calculates matrix elements involving more than one final continuum particle exactly.

ACKNOWLEDGMENTS

We wish to thank Marshall Blann for many useful discussions, and in particular for suggesting that multiple preequilibrium emission can be determined from much of the existing primary FKK theory. We also gratefully acknowledge useful conversations with G. Arbanas, A. Cowley, F. Dietrich, A. Kerman, A. Koning, D. Madland, J. Pilcher, and H. Weidenmuller. This work was performed in part under the auspices of the U.S. Department of Energy by Lawrence Livermore National Laboratory under Contract No. W-7405-Eng-48, and by Los Alamos National Laboratory under Contract No. W-7405-Eng-36.

[1] H. Feshbach, A. Kerman, and S. Koonin, Ann. Phys. (N.Y.) **125**, 429 (1980).
[2] D. Kielan, A. Marcinkowski, and U. Garuska, Nucl. Phys. **A 559**, 333 (1993).
[3] A. Marcinkowski, J. Rapaport, R.W. Finlay, C. Brient, M. Herman, and M.B. Chadwick, Nucl. Phys. **A561**, 387 (1993).
[4] W.A. Richter, A.A. Cowley, G.C. Hillhouse, J.A. Standers, J.W. Koen, S.W. Steyn, R. Lindsay, R.E. Julies, J.J. Lawrie, J.V. Pilcher, and P.E. Hodgson, Phys. Rev. C **49**, 1001 (1994).
[5] S. Stamer, W. Scobel, W.B. Amian, R.C. Byrd, R.C. Haight, J.L. Ullmann, R.W. Bauer, M. Blann, B.A. Pohl, J. Bisplinghoff, and R. Bonetti, Phys. Rev. C **47**, 1647 (1993).
[6] A.J. Koning and J.M. Akkermans, Phys. Rev. C **47**, 724 (1993); A. Koning, in *Proceedings of the Symposium on Nuclear Data Evaluation Methodology*, Brookhaven National Laboratory, Upton, New York, 1992, edited by C. Dunford (World Scientific, Singapore, 1993), p. 434.
[7] M.B. Chadwick and P.G. Young, Phys. Rev. C **47**, 2255 (1993); M.B. Chadwick and P.G. Young, in *Proceedings of the Symposium on Nuclear Data Evaluation Methodology* [6], p. 424.
[8] M.B. Chadwick and P.G. Young, in *Proceedings of the Workshop on Simulating Accelerator Radiation Environments*, Santa Fe, 11-15 January 1993 (World Scientific, in press).
[9] M.B. Chadwick, P.G. Young, A. Marcinkowski, and P. Oblozinsky, Phys. Rev. C **49**, R2885 (1994).
[10] M.B. Chadwick and P.G. Young, Los Alamos Document LA-UR-93-104, 1993 (unpublished).
[11] M. Avrigeanu, P.E. Hodgson, A.J. Koning, J. Phys. G **19**, 745 (1993); P. Demetriou, P. Kanjanarat, and P.E. Hodgson, *ibid.* **19**, L193 (1993).
[12] J.M. Akkermans and H. Gruppelaar, Z. Phys. A **300**, 345 (1981).
[13] M. Blann and H. Vonach, Phys. Rev. C **28**, 1475 (1983).
[14] S.V. Fortsch, A.A. Cowley, J.J. Lawrie, J.V. Pilcher, F.D. Smit, and D.M. Whittal, Phys. Rev. C **48**, 743 (1993).
[15] G. Ciangaru, Phys. Rev. C **30**, 479(1984).
[16] J.V. Pilcher, A.A. Cowley, D.M. Whittal, and J.J. Lawrie, Phys. Rev. C **40**, 1937 (1989).
[17] R. Bonetti, M.B. Chadwick, P.E. Hodgson, B.V. Carlson, and M.S. Hussein, Phys. Rep. **202(4)**, 171 (1991).
[18] M.B. Chadwick, Los Alamos National Laboratory Document LA-UR-92-2346, 1992 (unpublished).
[19] C.D. Bowman *et al.*, Nucl. Instrum. Methods **A320**, 336 (1992).
[20] A.J. Koning, Nuclear Energy Agency document NEA/NSC/Doc(92)12, 1993 (unpublished); NEA/NSC/Doc(93)6, 1993 (unpublished).
[21] H.M. Blann, H. Gruppelaar, P. Nagel, and J. Rodens, Nuclear Energy Agency Document NSC/DOCS(93)8, 1993 (unpublished).
[22] F. C. Williams, Nucl. Phys. **A166**, 231 (1971); E. Betak and J. Dobes, Z. Phys. A **279**, 319 (1976); P. Oblozinsky Nucl. Phys. **A453**, 127 (1986).

[23] H. Feshbach, Phys. Rev. C **48**, R2553 (1993); H. Feshbach, Ann. Phys. (N.Y.) **159**, 150 (1985).
[24] A.J. Koning and J.M. Akkermans, Ann. Phys. (N.Y.) **208**, 216 (1991).
[25] L. Avaldi, R. Bonetti, and L. Colli-Milazzo, Phys. Lett. **94B**, 463 (1980).
[26] M. Blann, in *Proceedings of a Specialists' Meeting on Preequilibrium Reactions*, Semmering, Austria, 10–12 February 1988, edited by B. Strohmaier (OECD, Paris, 1988), p. 171.
[27] H. Vonach, A. Pavlik, M.B. Chadwick, R.C. Haight, R.O. Nelson, and P.G. Young [Phys. Rev. C (to be submitted)]; P.G. Young, M.B. Chadwick and M. Bozoian, in *Proceedings of the Symposium on Nuclear Data Evaluation Methodology* [6] p. 480.
[28] W.A. Richter, A.A. Cowley, R. Lindsay, J.J. Lawrie, S.V. Fortsch, J.V. Pilcher, R. Bonetti, and P.E. Hodgson, Phys. Rev. C **46**, 1030 (1992).
[29] P.D. Kunz, DWUCK4 code, University of Colorado (unpublished).
[30] H. Weidenmuller, private communication to M.B. Chadwick, 1992.
[31] P.G. Young, E.D. Arthur and M.B. Chadwick, Los Alamos National Laboratory Report No. LA-12343-MS 1992 (unpublished).
[32] O. Bersillon, in *Progress Report of the Nuclear Physics Division, Bruyeres-le-Chatel 1977*, Bruyeres-le-Chatel Document CEA-N-2037, 1978 p. 111.
[33] H. Gruppelaar, in *IAEA Advisory Group Meeting on Basic and Applied Problems on Nuclear Level Densities*, edited by M.R. Bhat (Brookhaven National Laboratory, Brookhaven, N.Y., 1983), p. 143.
[34] R.L. Walter and P.P. Guss, in *Nuclear Data for Basic and Applied Science*, Santa Fe, 1985, edited by P.G. Young (Gordon and Breach, N.Y., 1986), p. 1079.
[35] P. Schwandt, H.O. Meyer, W.W. Jacobs, A.D. Bacher, S.E. Vigdor, M.D. Kaitchuck, and T.R. Donoghue, Phys. Rev. C **26**, 55 (1982).
[36] D.G. Madland, in *Proceedings of a Specialists' Meeting on Preequilibrium Reactions*, Semmering, Austria, 10-12 February 1988, edited by B. Strohmaier (OECD, Paris, 1988), p. 103; International Atomic Energy Agency Report No. IAEA-TECDOC-483, 1988, p. 80 (unpublished).
[37] P.A. Seeger and R.C. Perisho, Los Alamos Report No. LA-3751, 1967 (unpublished).
[38] F.E. Bertrand and R.W. Peelle, Phys. Rev. C **8**, 1045 (1973).
[39] C. Kalbach, Z. Phys. A **283**, 401 (1977).
[40] A.V Ignatyuk, G.N. Smirenkin, and A.S. Tishin, Sov. J. Nucl. Phys. **21**, 255 (1975).
[41] E.D. Arthur, Nucl. Sci. Eng. **76**, 137 (1980).
[42] S. Watanabe, Nucl. Phys. **8**, 484 (1958).
[43] J. Kopecky and M. Uhl, Phys. Rev. C **42**, 1941 (1990).
[44] As an illustrative example, the spectral shape for N=1 multiple preequilibrium can be obtained analytically if some simplifying assumptions are made. Suppose that the first-stage primary MSD spectrum is constant in energy, and that the transmission coefficient is unity. Then Eq. (5) yields an $N = 1$ multiple shape $\propto c$ for $E > \epsilon_F - B$ and $\propto c(E + B)/\epsilon_F + c\ln(\epsilon_F/E + B)$, for $E < \epsilon_F - B$, where c is a constant, as approximately seen in Fig. 3. Deviations from this shape for large energies are due to the deviations from a constant primary spectrum, and for low energies are due to the effect of the transmission coefficient.
[45] A.M. Kalend *et al.*, Phys. Rev. C **28**, 105 (1983).
[46] M. Trabandt, W. Scobel, M. Blann, B.A. Pohl, R.C. Byrd, C.C. Foster, and R. Bonetti, Phys. Rev. C **39**, 452 (1989).
[47] Y. Watanabe, M. Avrigeanu, and W.A. Richter, Oxford University Document No. OUNP-93-30, 1993 (unpublished).
[48] W. Scobel, M. Trabandt, M. Blann, B.A. Pohl, B.R. Remington, R.C. Byrd, C.C. Foster, R. Bonetti, C. Chiesa, and S.M. Grimes, Phys. Rev. C **41**, 2010 (1990).
[49] A.A. Cowley, A. van Kent, J.J. Lawrie, S.V. Fortsch, D.M. Whittal, J.V. Pilcher, F.D. Smit, W.A. Richter, R. Lindsay, I.J. van Heerden, R. Bonetti, and P.E. Hodgson, Phys. Rev. C **43**, 678 (1991).